

PAPER • OPEN ACCESS

## Laser machining of sensing components on the end of optical fibres

To cite this article: Frank Albri *et al* 2013 *J. Micromech. Microeng.* **23** 045021

View the [article online](#) for updates and enhancements.

### You may also like

- [Fabricating optical fibre-top cantilevers for temperature sensing](#)  
J Li, F Albri, J N Sun et al.
- [Surface quality and morphology of NiTiCuZr shape memory alloy machined using thermal-energy processes: an examination of comparative topography](#)  
C Balasubramaniyan, S Santosh and K Rajkumar
- [Trimming for alumina-based ceramic casting cores for turbine blade by double picosecond laser scanning](#)  
Chaoqing Min, Quansheng Li, Xianbin Yang et al.

# Laser machining of sensing components on the end of optical fibres

Frank Albri, Jun Li, Robert R J Maier, William N MacPherson and Duncan P Hand

Institute of Photonics and Quantum Sciences, SUPA, School of Engineering and Physical Sciences, Heriot-Watt University, Edinburgh, EH14 4AS, UK

E-mail: [fa192@hw.ac.uk](mailto:fa192@hw.ac.uk) and [d.p.hand@hw.ac.uk](mailto:d.p.hand@hw.ac.uk)

Received 21 December 2012, in final form 12 February 2013

Published 7 March 2013

Online at [stacks.iop.org/JMM/23/045021](http://stacks.iop.org/JMM/23/045021)

## Abstract

Micro-cantilevers play a major role in sensing, especially since the invention of the atomic force microscope. Applications range from surface profiling to bio-medical sensing enabled through coating-activated cantilevers. Current readout methods are based on either optical deflection (of a laser beam reflected from the cantilever surface) or piezo-resistive response (of piezo-electric elements bonded to the cantilever surface). The first of these approaches requires significant space whilst the second is sensitive to electromagnetic effects. An alternative solution is to manufacture a cantilever onto the end of an optical fibre and use interferometry to monitor its deflection; in this paper we describe the development and application of a picosecond-laser machining process to fabricate such a device. The development of techniques to avoid cracking and debris re-deposition during this machining process is described, and a cantilever sensor with excellent optical performance is demonstrated and tested.

(Some figures may appear in colour only in the online journal)

## 1. Introduction

Cantilever structures for sensing applications have a proven and highly successful track record. They are successfully used as the basis of the atomic force microscope (AFM) where the probe tip is attached to a micro-cantilever [1] to allow a measure of test surface profile with 0.1 nm resolution. However by adding a specific coating on one side of the cantilever [2–4] it is possible to sensitize the cantilever to temperature, chemical or bio-chemical species. Therefore there is considerable interest in using micro-cantilevers in a wide range of measurement applications.

Cantilever readout methods currently used are either (i) optical beam deflection where a laser beam is directed onto one side of the cantilever and the change of angle in the reflected beam is detected [5] or (ii) on-cantilever piezo-resistive strain gauges [6]. The beam deflection technique is more commonly used and, although insensitive to electromagnetic fields, it does require good optical access to the cantilever to allow the deflection to be measured. Since the sensitivity of this measurement scales with the length of the ‘optical lever’ it is not straightforward to miniaturize the interrogation system. Piezo-resistive sensors can be fabricated onto the cantilever,

but are unsuitable for use in electromagnetic environments or in conductive media.

A cantilever sensor that overcomes these shortcomings was designed by Iannuzzi *et al* [7, 8], where the cantilever is carved onto the end face of a fused silica optical fibre. A Fabry–Perot cavity is formed between the cantilever and the end face of the fibre, the length of which can be accurately measured (in our case with a resolution down to 15 nm) by a remote optical interrogation system located at the other end of the fibre. Formation of the optical cavity relies on reflections from machined surfaces, and so the surface roughness should be as low as possible to ensure sufficient optical signal is returned to the interrogation system. Therefore the machining process must be carefully optimized to minimize roughness. Another important factor is the relative angles of the surfaces. They must be sufficiently parallel to each other, and also perpendicular to the fibre axis to ensure that the reflected signal is coupled back into the fibre core. An angular deviation of up to  $\sim 3^\circ$  can be tolerated due to the divergence of the light exiting the fibre and the associated acceptance angle (numerical aperture).

Cantilever fibre sensors have been reported elsewhere based upon fabrication using focussed ion beam (FIB) milling.



This can create very thin and delicate cantilevers, with dimensions as small as  $1.3 \mu\text{m}$  reported in [7]. The associated surface finish is excellent with typical roughness of less than  $10 \text{ nm RMS}$  [9]. However the major shortcoming of this manufacturing technique is the time and cost required to manufacture a single sensor. Due to the low material removal rate of the FIB process [10] it can take up to 4 h on an expensive facility to produce a single sensor [11]. This has limited the application of such sensor devices to high value scientific applications. Iannuzzi, who presented the first FIB machined fibre-top cantilever, has also investigated the application of femtosecond laser assisted etching. This technique can produce elaborate sub-micron scale features and has been reported for the generation of buried channels in fused silica [12–15]. While this process improves the machining time, it still took about 90 min to manufacture the first set of prototypes although further improvements could be achieved by parallel production. However the surface roughness does not match the FIB machined surfaces, and the minimum cantilever thickness is about  $20 \mu\text{m}$ . A very promising technique to mass manufacture a cantilever structure onto the end of the fibre was developed by Gavan *et al* who use a lithographic process of applying a photoresist, transfer of a pattern, development, deposition of a gold-chromium bilayer and lift off of the photoresist followed by wet etching to release the cantilever from the fibre [16].

An alternative technology would be micro powder blasting. Unfortunately the aspect ratios are limited [17–21] with the best that can be achieved around 2.5:1 [17] which is insufficient for cantilever designs. Furthermore the current minimum feature sizes (typically  $50 \mu\text{m}$ ) remain too large for such intricate structures.

In this paper we discuss a new approach to manufacture micro-cantilever structures onto the end of an optical fibre by direct laser ablation using a commercial picosecond (ps)-laser system. We demonstrate a process that easily adapts to mass manufacturing whilst generating cantilevers of appropriate quality and optical performance to enable sensing applications. This technique has shown promising results on larger cantilever sensors that were carved out of borosilicate glass ferrules and for which several applications have already been demonstrated [22, 23].

The results presented and discussed in this paper are applicable to a much wider range of structures and features manufactured from fused silica. This indicates the potential of ps-laser processing to augment micro manufacturing of an otherwise difficult to machine material.

## 2. Cantilever fabrication

Laser processing has seen significant development and is commercially used for a wide range of applications including welding, cutting, and drilling. The choice of laser depends upon many factors including material absorption and desired feature size. For features with a scale of a few micrometres in fused silica, we choose to use a picosecond laser operating in the ultra violet region. The wavelength of operation maximizes the absorption of the laser radiation, and allows for a tight

focus, while picosecond operation allows controllable delivery of optical power. Details of the fabrication process are given in the following sections.

### 2.1. Picosecond-laser machining facility

The laser machining workstation is centred around a commercial ps-laser (Trumpf TruMicro 5050 3C) emitting pulses around 6 ps, with a wavelength of 343 nm, repetition rate of up to 400 kHz and maximum pulse energy of  $35 \mu\text{J}$ . The beam is expanded to a diameter of 14 mm to match the aperture of a galvanometer scan head which is equipped with a 160 mm focal length f-theta lens. The beam waist at focus is measured using the knife edge measurement to have an  $e^{-2}$  waist radius of  $w_0 = 7 \pm 1 \mu\text{m}$  (limited by the accuracy of the measurement system). During machining, the beam is scanned across the work piece by means of this scan head. For all results presented in this paper, the scan speed and laser repetition rate are kept constant at  $100 \text{ mm s}^{-1}$  and 40 kHz, respectively, resulting in a spot-to-spot displacement of  $2.5 \mu\text{m}$ . In cases where the laser is scanned through a number of parallel lines (in order to machine across an area), the line spacing used is  $4 \mu\text{m}$  to provide the most uniform material removal. The repeatability of the scan heads is better than  $22 \mu\text{rad}$  [24] which in the working plane resulted in a beam position accuracy of better than  $2.8 \mu\text{m}$ .

A high precision 4-axis system is used for workpiece positioning, consisting of three orthogonal linear axes plus one rotational axis for precise control of machining angles. The stages are also used to move the sample to an inspection microscope for immediate analysis and to act as a positioning aid to ensure correct registration between the workpiece and the laser machining datum. This is possible with a  $\pm 15 \mu\text{m}$  in the focusing direction ( $z$  direction). In a repeatability test we moved the sample between the machining area and the microscope ten times and had a positioning error of  $\pm 1.8 \mu\text{m}$  laterally ( $x$ - $y$  plane) from the average centre. This is sufficient for our purpose as the critical alignment between the fibre core and cantilever machining location needs to be better than the core diameter ( $< 10 \mu\text{m}$ ) to ensure overlap between the core and final cantilever structure. The Rayleigh range of the focussed laser is  $Z_R = 295 \pm 90 \mu\text{m}$  which is well within the focussing accuracy therefore ensuring the workpiece is in the correct portion of the beam.

### 2.2. Optimized laser parameters

Fused silica can be a challenging material to laser-process, with cracking being a particular problem, which can significantly weaken a structure. Key parameters are the ablation thresholds for fused silica for both single and multiple pulses. These are determined experimentally using a fused silica microscope slide. An array of machined points generated with differing pulse energies allows the ablation threshold to be determined [25–28]. The ablation thresholds are found to be  $2.8 \text{ Jcm}^{-2}$  for single laser shots and  $0.9 \text{ Jcm}^{-2}$  for 100 shots.

Irradiating the sample with energy densities below the single shot surface ablation threshold still modifies the bulk of the material (presumably due to self-focusing) and causes

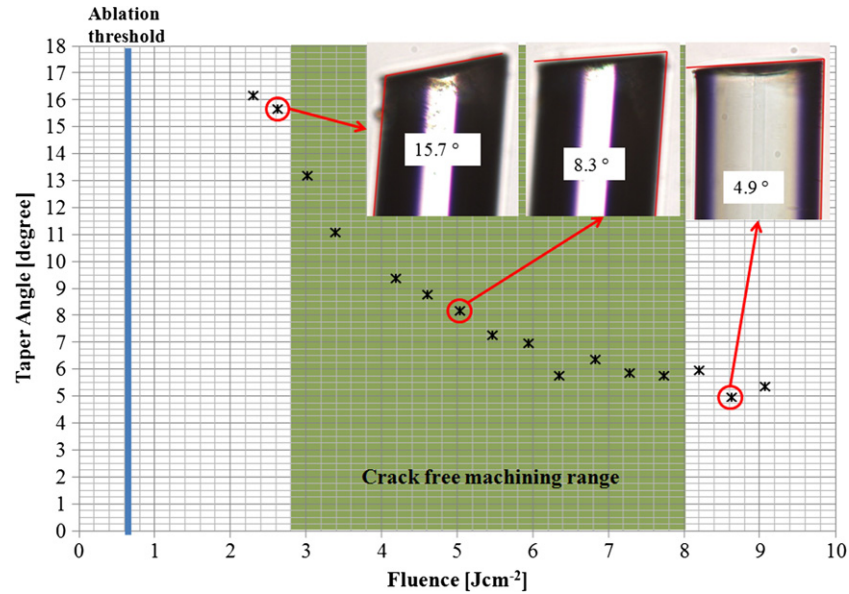


**Figure 1.** Taper angle as a function of laser fluence. The optimum machining range is highlighted, in which the fluence is sufficient to achieve surface ablation rather than bulk damage whilst not being so high as to cause cracking of the fibre. Inset figures show microscope images of fibres cut with the laser at different fluences illustrating the difference in taper angle.

many cracks, both internally and at the surface. For pulse energies in excess of approximately  $9.0 \text{ Jcm}^{-2}$  significant cracking is observed on the surface, probably due to excess energy being deposited in the material causing stress and shockwaves. For the manufacture of thin and narrow structures as is required for cantilevers, it is essential to avoid all such cracking, and so the processing window has been defined as being between  $2.6$  and  $8.0 \text{ Jcm}^{-2}$ , as shown in figure 1.

### 2.3. Taper angle

In common with many other laser machining processes [29–32], the machined features are tapered. This angle is strongly dependent on the laser fluence, as illustrated in figure 1. In order to minimize the introduction of stress an energy fluence at the lower end of the processing window,  $3.5 \text{ Jcm}^{-2}$ , is chosen for cantilever manufacture, giving a taper angle of roughly  $10^\circ$ . Furthermore the lower fluence also minimizes the amount of material debris re-deposition.

### 2.4. Manufacturing approach

The manufacturing approach shown schematically in figure 2 was established as a result of significant experimentation, in order to minimize the debris deposition onto important surfaces and to avoid cracking. This requires four discrete machining steps which are carried out using a single setup and so has potential for automation. In step one, a ridge is established at the end of the fibre (figures 2(a) and (b)). A through cut is then made to form the cantilever with a surface parallel to the end face of the fibre (figures 2(c) and (d)). A further through cut forms the second face of the optical cavity, with the workpiece appropriately rotated to ensure the surface is perpendicular to the fibre axis (figures 2(e) and (f)). A final cut is made to remove the small debris catching structure between the first two cuts (figures 2(g) and (h)). Key features in

the development of this process are described in the following sections.

**2.4.1. Establishing a ridge on a fibre end face.** Prior to the actual machining process, the fibre is cleaved using an optical fibre cleaver which generates a near ideal optically smooth surface, normal to the longitudinal fibre axis. The fibre was mounted into a v-groove attached to the 4-axis positioning system with a short length of fibre protruding from the mount. This system was used to position the cleaved fibre surface perpendicular to the incident laser beam. The first step in the manufacturing process is to establish a ridge on the end of the fibre, which is subsequently modified into a cantilever structure. The scan head is then used to translate the focused laser spot across this surface removing the outer parts of the fibre as shown in figure 3. By repeating this scan pattern, subsequent layers are removed from the cleaved surface of the fibre leaving only a ridge in the centre of the fibre standing, resulting in a shape very similar to a flat bladed screw driver tip. An illustration of how the shape of the ridge evolves through several repetitions of the scanning pattern is shown in figure 4.

**2.4.2. Establishing a cantilever.** The next processing step is to remove material underneath the end face of the ridge to establish a free standing cantilever (figure 2(d)). In order to achieve this the fibre is rotated by  $100^\circ$ , i.e.  $90^\circ$  to gain access to side of the ridge to allow removal of material underneath the cleaved surface and an additional  $10^\circ$  to compensate for the taper angle and machine a surface parallel to the cleaved end of the fibre. A further machining process is then necessary to remove the  $20^\circ$  taper on the other face of the cut, achieved by rotating the fibre by  $20^\circ$ ; however to prevent debris being deposited on the inside of the cantilever this is carried out in two steps (figures 2(e) and (g)). The final cut (figure 2(g)) to remove the central structure is very short and little debris is generated.

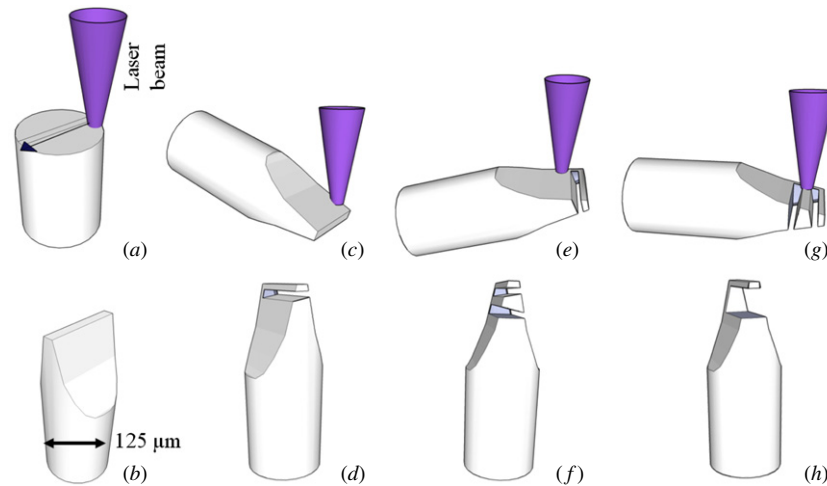


**Figure 2.** Steps of the laser manufacturing process to establish a cantilever onto the end of an optical fibre. Focussed laser beam indicated by purple cone.

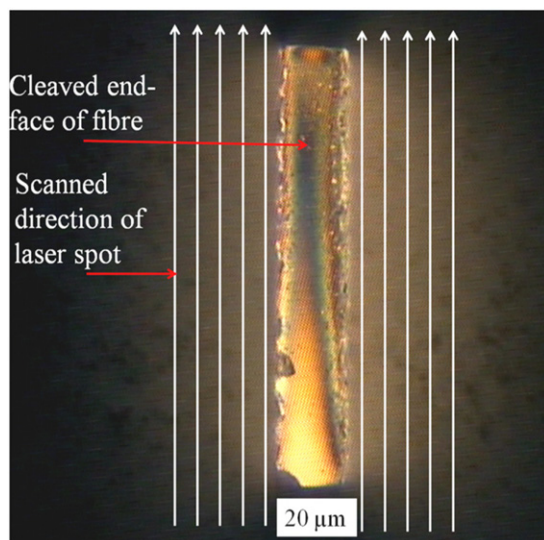


**Figure 3.** End face of a cleaved fibre machined using the laser. Arrows indicate direction of single lines across the surface of the fibre.

2.5. Minimizing debris

During laser machining a common problem is the deposition of debris, on surfaces in the vicinity of the ablation process. This debris is generated from a spray of material removed as very small molten droplets, together with vaporized material re-condensing [33]. In some cases this debris is bonded very weakly to the surface in which case it is easily removed by sonication; however it can also be welded to the surface and hence almost impossible to remove except by a polishing process. This accumulation of debris decreases the optical quality of surfaces due to random scattering, resulting in a reduction in the reflected optical intensity. In the work reported here, ultrasonic cleaning or air jet debris removal has been only partially successful.

The location of the re-deposited debris strongly depends on the physical constraints created by surfaces in the vicinity of a cut, so machining approaches can have significant impact

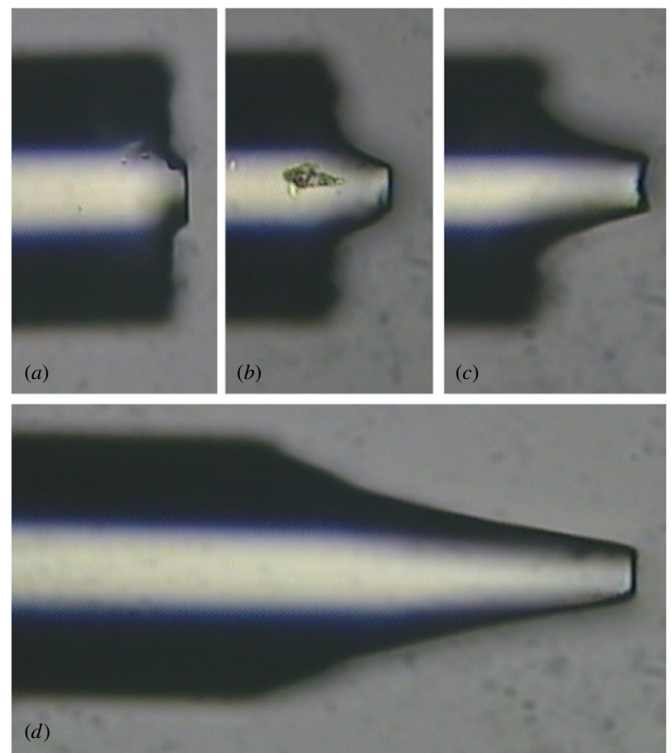


**Figure 4.** Evolution of ridge shape through various repetitions of laser machining pattern keeping consistent constant focal plane and a fluence of  $0.9 \text{ J cm}^{-2}$ : (a) once; (b) 5 times; (c) 10 times; (d) 25 times.

on debris deposition patterns. Therefore it is essential to design machining sequences to avoid directing debris towards any of the critical surfaces, i.e. those which interact with the optical signal. During the first step of laser machining, establishing the ridge, it is important to minimize debris deposition on the cleaved fibre surface which will later form the outside of the cantilever. Figure 5 illustrates the simplest pattern that results in a uniform material removal on both sides of the ridge; however in figure 5(b) it is clear that the deposition of debris

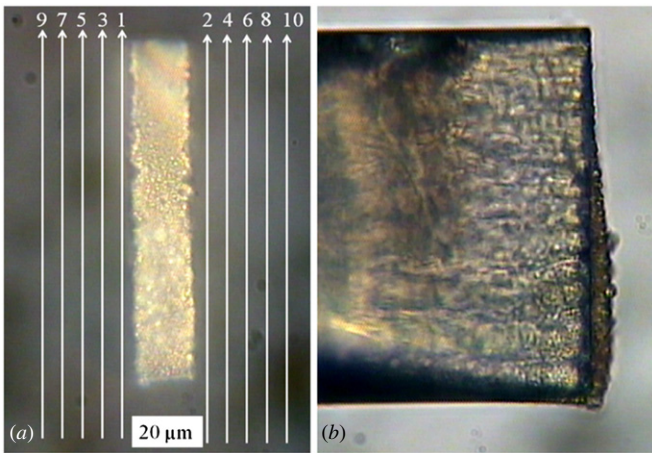


**Figure 5.** Scanning the laser beam in one direction over the end face of the cleaved fibre resulting in the ridge structure with non-uniform deposition of debris. (a) View of the machined end face of the fibre and (b) view from the side showing a thicker layer of debris on the beginning of the machining process.

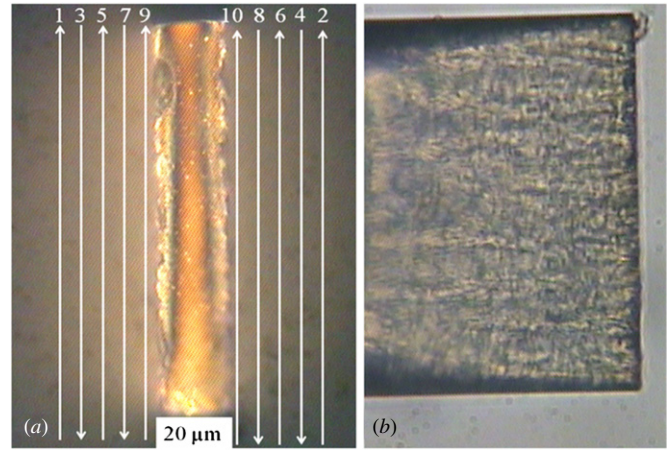


**Figure 7.** Optimal scanning approach for lowest debris deposition. Scanning is carried out from the outside, moving into the centre; also the scanning direction was alternated. Microscope images of the machined ridge structure (a) from top with indication of movement of the spot; (b) view from the side showing low deposition of debris.

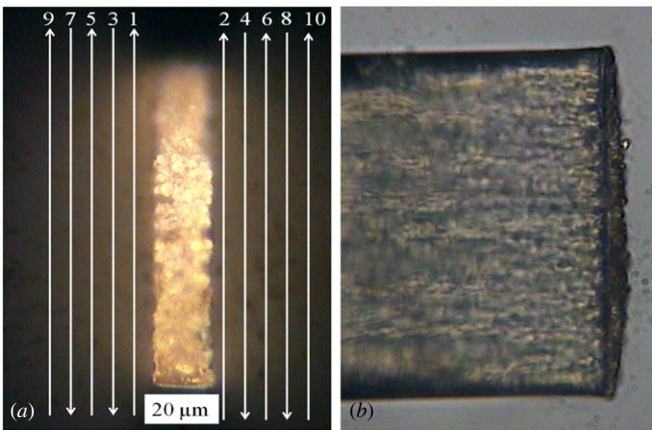


**Figure 6.** Scanning approach to generate uniform debris deposition, by alternating the direction in which the laser is scanned. The machining process was started next to the ridge. (a) View of the end face of the machined ridge; (b) side view showing deposited layer of debris.

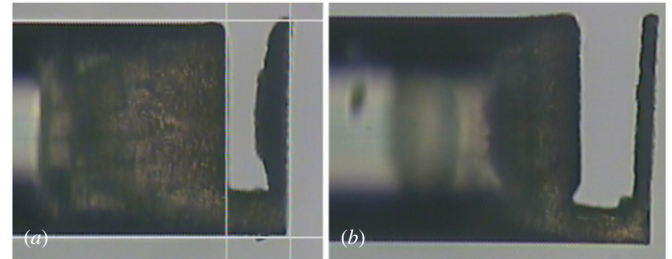


**Figure 8.** Comparison of a cantilever machined (a) without sacrificial structure to catch debris and (b) with this structure.

has taken place with a layer of up to 10  $\mu\text{m}$  thick debris, with maximum thickness at the beginning of the scanned lines.

By changing the scanning pattern to alternate the starting direction of each line, in a way that neighbouring scans point into opposite directions, as illustrated in figure 6, it is possible to achieve a more uniform deposition of debris; however the layer of deposited debris is still up to 8  $\mu\text{m}$ . The overall direction of the scans is from the inside towards the outside as indicated by the numbers in figure 6(a); however if this direction is changed as shown in figure 7(a) the deposition of debris is greatly reduced. This is due to the fact that the spray of particles will have less constraints away from the centre of the fibre.

### 2.6. Reduction of debris on the cantilever structure

To compensate for the taper angle, it is essential to machine each cut at an angle relative to the axis of the beam to establish

parallel surfaces. At least two cuts are therefore necessary to establish a cantilever, each made at a different angle to generate parallel faces. As discussed earlier in section 2.4.2, the second cut in this part of the process is made a distance away from the first cut in order to leave a sacrificial structure in between the cuts, to act as a barrier to prevent debris deposition on the inner surface of the cantilever. The sacrificial structure is then removed by a third small cut. The impact of this approach is demonstrated in figure 8, where (a) shows the significant debris deposited if no sacrificial structure is used, and (b) with the sacrificial structure. This sacrificial structure approach sets a practical lower limit to the separation between the newly formed fibre end face and the cantilever surfaces of around 25  $\mu\text{m}$ .

### 3. Post-fabrication surface arc-discharge smoothing

The laser machined surfaces have a high surface roughness of  $R_{\text{rms}} = 0.2 \mu\text{m}$ . This surface roughness causes scattering which reduces the optical return from the sensor. A typical reflection from a machined end face of a fibre is only 0.10% rather than the  $\sim 3.5\%$  expected from a Fresnel reflection. Even with such a low signal return from the optically active surfaces, cantilevers have been demonstrated to work as sensors; however the signal-to-noise is clearly much lower than it would be with

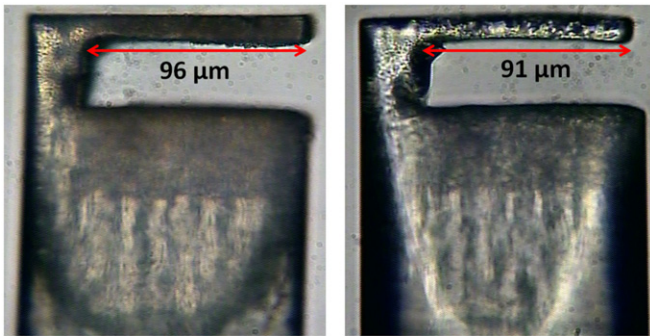


**Figure 9.** Laser machined fibre cantilever before (left) and after (right) cleaning and partially melting using an electric arc.

perfect optically smooth surfaces. Despite the low reflectivity, the fringe visibility of the cantilever interferometer is 0.80.

We therefore investigated thermal polishing to reduce the roughness by application of heat to the surface of the cantilever to cause localized melting and smoothing via surface tension effects. Our approach here is to use an electric arc fibre optic ‘fusion’ splicer (Beale International Technology BFS-50), commonly used for joining fibre optics. The splicer is used in the ‘cleaning’ mode, which is conventionally used for removing dust and particles from the optical fibres before splicing them together. A further advantage of this cleaning arc is that it will also remove weakly bonded debris from the surface of the fibre. Using an arc current of 11 mA with a duration of 1 s, we achieved an improvement in the signal intensity by over a factor of 10 resulting in a fringe visibility of 0.69. Examination of the fibre under a microscope (see figure 9 (right)) demonstrates that some partial melting has occurred on the surface of the cantilever and the fibre. This melting also causes a slight decrease in the length of the cantilever as well as a reduction of scatter and formation of other surface structures. Care must be taken when choosing the arc cleaning duration, too much heat leads to cantilever deflection away from the fibre, ultimately to the point where the angle is too large to get a sufficient return signal. In addition the cantilever becomes thicker and shorter (i.e. stiffer) which is detrimental for its intended sensing application.

By adopting this surface smoothing process we are able to fabricate robust cantilevers suitable for sensing applications.

#### 4. Cantilever displacement sensor

To demonstrate that the proposed process is capable of machining fused silica fibres to a quality sufficient for optical sensing, we manufactured a cantilever sensor with a thickness of 10 μm and a length of roughly 100 μm. This cantilever is tested as a simple displacement sensor. An actuator is used to push the end of the cantilever by a known distance and thereby displace it slightly. The response is observed using an optical microscope as well as a commercial interferometric displacement sensor (Renishaw ML10) capable of a measurement accuracy of 1 nm. The cantilever deflection is obtained by determining the optical cavity length via analysis of the spectrum of the reflected light [34].

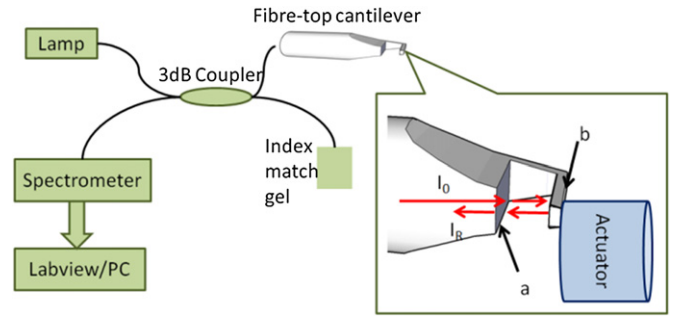


**Figure 10.** Fibre interrogation system.

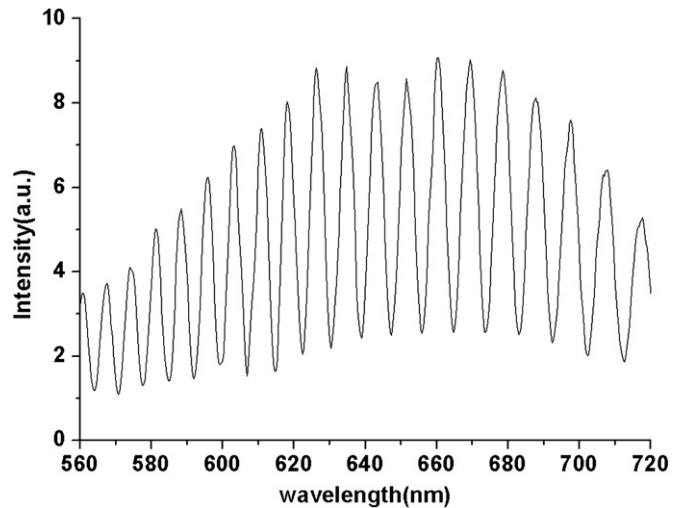


**Figure 11.** A typical spectrum recorded from a cantilever when illuminated by a tungsten light bulb through a 2 × 2 fibre optic coupler for 633 nm.

The optical interrogation system consists of a low-cost broadband light source (tungsten halogen lamp) and a grating-based CCD spectrometer (Ocean Optic S2000) with an integration time of 200 ms. A 3 dB fibre coupler for 633 nm is used to direct light reflected to and from the sensor cavity to the spectrometer. The light is partially reflected by the first surface of the cantilever which is the fibre-to-air interface (surface (a) in figure 10 inset). A second reflection occurs from the air-to-cantilever interface and a third reflection from the cantilever-to-air interface (surface (c) in figure 10 inset). The intensity of the light reflected by the air-to-cantilever interface (surface (b) in figure 10 inset) is very low due to surface roughness, and to a first approximation this reflection does not contribute significantly to the optical signal and therefore can be ignored. The main sensing interference is generated by the two remaining reflections, and the resulting channelled spectrum is recorded by the spectrometer. A typical reflection spectrum is shown in figure 11.

Cantilever displacement results in a change in the length of the optical cavity, and therefore the spectrum of the cavity reflection is modified. It is possible to extract the cavity length by analysing the spectrum, using a fast Fourier transform (FFT) technique [34]. The noise level is determined by mounting the cantilever in a temperature stabilized environment ( $\pm 1$  °C), and using the optical interrogation system to measure the

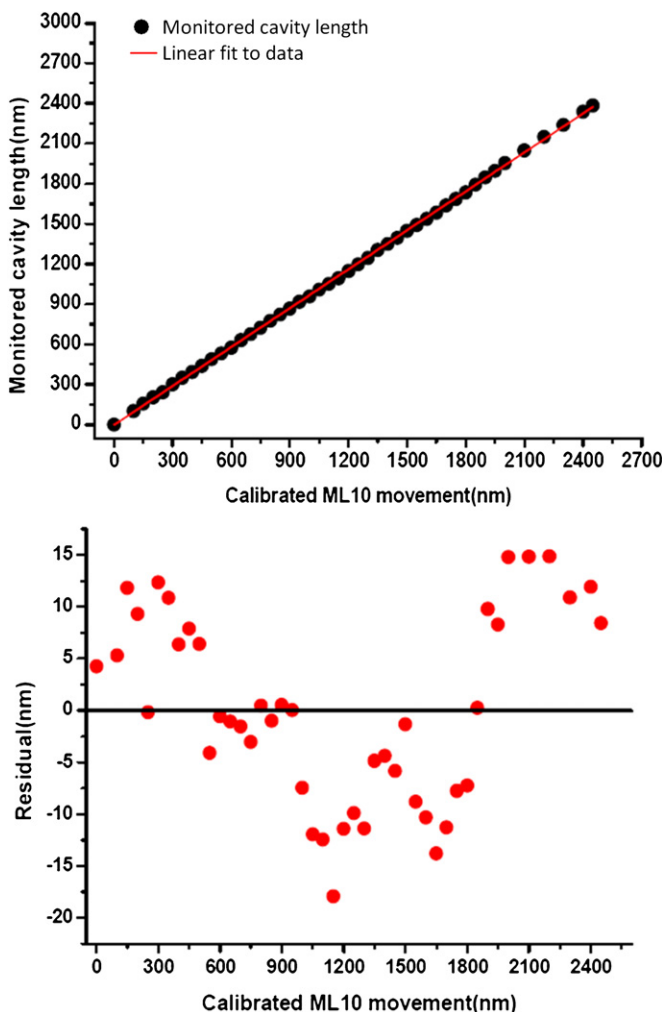


**Figure 12.** Cavity length measured with fibre optic interrogation method versus the measurement taken with a commercial displacement sensor and the residuals of a linear fit to the measurement data.

cavity length over a period of 5 min (measurement made every second). This showed a standard deviation of 16 nm. An overall drift test is made under similar conditions measuring over a 5 h time span showing a maximum deviation equivalent to 50 nm. For actuation testing the cantilever is mounted onto a micro block, with actuation applied via a second fibre controlled by a calibrated piezo-electric translation stage. It is possible to observe the deflection both through a microscope, and via the interrogation system. The actuation of the cantilever is independently measured using an optical displacement sensor. A plot of the data recorded using the fibre interrogation system and using the ML10 is shown in figure 12.

## 5. Conclusions

Picosecond laser manufacturing is suitable for directly machining interferometric micro-cantilever sensors into single mode optical fibres, provided that a suitable approach is used to minimize debris re-deposition onto the optically important surfaces. Compensation for the machining taper angle (by angling the fibre relative to the machining laser)

is essential to ensure that light reflected from the cantilever structure is coupled back into the optical fibre. We report the successful manufacture of complete and stable cantilever sensors and have shown that this structure can be actuated over a range of more than 3  $\mu\text{m}$ . Based on a rectangular profile,  $110 \times 20 \times 10 \mu\text{m}^3$ , a deflection of 3  $\mu\text{m}$  would result in a maximum surface strain of around 0.6%; operation without mechanical failure at this strain suggests that the cantilevers are free from cracks. However the thickness of the cantilever and the resulting spring constant reduce the range of applications of such a cantilever sensor.

The manufacturing process is easily adaptable into an industrial manufacturing process. The total time of active laser processing, i.e. laser-on time, is less than 30 s for each cantilever. This shows promise towards large-scale mass manufacturing. For example, the beam could be split into several parts capable of processing up to three fibres at the same time; also a higher speed scanner would allow the laser pulse repetition rate to be increased. By combining both of these approaches, it would be possible to manufacture 20 cantilevers per minute using our picosecond laser. Even when using purely manual handling, from fibre cleaving to manual alignment of the fibre with respect to the laser, the process took less than 6 min per cantilever, which is significantly shorter than any other reported manufacturing method for this type of structure.

## Acknowledgments

The authors would like to thank the Innovative Manufacturing Research Centre (IMRC) and the Engineering and Physical Research Council (EPSRC grant no. EP/F02553X/1) and Renishaw plc for partial funding of this project, as well as the Scottish Universities Physics Alliance for provision of a studentship for JL.

## References

- [1] Binnig G, Quate C F and Gerber C 1986 Atomic force microscope *Phys. Rev. Lett.* **56** 930–3
- [2] Lehenkari P P *et al* 2000 Adapting atomic force microscopy for cell biology *Ultramicroscopy* **82** 289–95
- [3] Ziegler C 2004 Cantilever-based biosensors *Anal. Bioanalytical Chem.* **379** 946–59
- [4] Raiteri R *et al* 2001 Micromechanical cantilever-based biosensors *Sensors Actuators B* **79** 115–26
- [5] Meyer G and Amer N M 1988 Novel optical approach to atomic force microscopy *Appl. Phys. Lett.* **53** 1045  
Meyer G and Amer N M 1988 Novel optical approach to atomic force microscopy *Appl. Phys. Lett.* **53** 2400–2 (erratum)
- [6] Tortonese M, Barrett R C and Quate C F 1993 Atomic resolution with an atomic force microscope using piezoresistive detection *Appl. Phys. Lett.* **62** 834–6
- [7] Iannuzzi D *et al* 2007 Fibre-top cantilevers: design, fabrication and applications *Meas. Sci. Technol.* **18** 3247–52
- [8] Iannuzzi D *et al* 2006 Monolithic fiber-top sensor for critical environments and standard applications *Appl. Phys. Lett.* **88** 053501
- [9] Li W X *et al* 2007 A study of fused silica micro/nano patterning by focused-ion-beam *Appl. Surf. Sci.* **253** 3608–14



- [10] Geil B 1993 Focused-ion-beam material removal rates *Summary Report Army Research Lab.* (Adelphi, MD: USAR)
- [11] Fu Y Q and Ngoi K A B 2004 Focused ion beam direct fabrication of micro-optical elements: features compared with laser beam and electron beam direct writing *Innovation in Manufacturing Systems and Technology* (IMST)
- [12] Gattass R R and Mazur E 2008 Femtosecond laser micromachining in transparent materials *Nat. Photon.* **2** 219–25
- [13] Said A A et al 2008 Carving fiber-top cantilevers with femtosecond laser micromachining *J. Micromech. Microeng.* **18** 035005
- [14] Madani-Grasset F and Bellouard Y 2010 Femtosecond laser micromachining of fused silica molds *Opt. Express* **18** 21826–40
- [15] Rajesh S and Bellouard Y 2010 Towards fast femtosecond laser micromachining of fused silica: the effect of deposited energy *Opt. Express* **18** 21490–7
- [16] Gavan K B et al 2011 Top-down approach to fiber-top cantilevers *Opt. Lett.* **36** 2898–900
- [17] Wensink H et al 2000 High resolution powder blast micromachining *13th Annu. Int. Conf. on Micro Electro Mechanical Systems, 2000 (MEMS 2000)* pp 769–74
- [18] Jung W C et al 2007 Micro machining of injection mold inserts for fluidic channel of polymeric biochips *Sensors* **7** 1643–54
- [19] Solignac D et al 2001 Powder blasting for the realisation of microchips for bio-analytic applications *Sensors Actuators A* **92** 388–93
- [20] Belloy E, Sayah A and Gijs M A M 2000 Powder blasting for three-dimensional microstructuring of glass *Sensors Actuators A* **86** 231–7
- [21] Hiromasa Y et al 2005 Micropowder blasting with nanoparticles dispersed polymer mask for rapid prototyping of glass chip *J. Micromech. Microeng.* **15** 1236
- [22] Gruca G et al 2010 Ferrule-top micromachined devices: design, fabrication, performance *Meas. Sci. Technol.* **21** 094033
- [23] Zuurbier P et al 2011 Measurement of the Casimir force with a ferrule-top sensor *New J. Phys.* **13** 023027
- [24] Scanlab A G 2011 hurrySCAN, hurrySCAN II technical data sheet SCANLAB AG <http://www.scanlab.de>
- [25] Ashkenasi D et al 1997 Pulse-width influence on laser structuring of dielectrics *Nucl. Instrum. Methods Phys. Res. B* **122** 359–63
- [26] Rosenfeld A et al 1999 Ultrashort-laser-pulse damage threshold of transparent materials and the role of incubation *Appl. Phys. A* **69** S373–6
- [27] Machado L M et al 2012 D-Scan measurement of ablation threshold incubation effects for ultrashort laser pulses *Opt. Express* **20** 4114–23
- [28] Ben-Yakar A and Byer R L 2004 Femtosecond laser ablation properties of borosilicate glass *J. Appl. Phys.* **96** 5316–23
- [29] Dubey A K and Yadava V 2008 Experimental study of Nd:YAG laser beam machining—an overview *J. Mater. Process. Technol.* **195** 15–26
- [30] Schaeffer R D Understanding and controlling taper when laser machining *Micro Manufacturing (Don Nelson 2010)* pp 13–4
- [31] Ghoreishi M, Low D K Y and Li L 2002 Comparative statistical analysis of hole taper and circularity in laser percussion drilling *Int. J. Machine Tools Manuf.* **42** 985–95
- [32] Yilbas B S 1997 Parametric study to improve laser hole drilling process *J. Mater. Process. Technol.* **70** 264–73
- [33] Shirk M D and Molian P A 1998 A review of ultrashort pulsed laser ablation of materials *J. Laser Appl.* **10** 18–28
- [34] Yi J 2008 Fourier transform white-light interferometry for the measurement of fiber-optic extrinsic Fabry-Perot interferometric sensors *IEEE Photon. Technol. Lett.* **20** 75–7